J|A|C|S COMMUNICATIONS

Published on Web 12/15/2009

Rhodium(0) Metalloradicals in Binuclear C−H Activation

Florian F. Puschmann,[‡] Hansjörg Grützmacher,*[,‡] and Bas de Bruin*[,†]

van't Hoff Institute for Molecular Sciences (Homogeneous and Supramolecular Catalysis Group) and Department of Chemistry, Universiteit van Amsterdam, Nieuwe Achtergracht 166, 1018 WV Amsterdam, The Netherlands, and Department of Chemistry and Applied Biology, ETH-Hönggerberg, CH-8093 Zürich, Switzerland

Received October 30, 2009; E-mail: gruetzmacher@inorg.chem.ethz.ch; b.debruin@uva.nl

The development of effective strategies for selective hydrocarbon activation and functionalization continues to be one of the major synthetic challenges. Generally applicable methods do not exist, and each of the known methods has its limitations or disadvantages.[1] Less conventional approaches are thus welcome. An interesting one consists of the use of two metalloradicals, as depicted in Scheme 1.

This concept has been scarcely explored. Wayland and coworkers reported the use of porphyrinatorhodium(II) complexes, [Rh^{II}(por)], which are capable of breaking C−H bonds of unactivated substrates, even methane.[2] These metalloradicals are proposed to activate the substrates via a binuclear transition state formed in a termolecular reaction in which one [Rh^{II}(por)] radical accepts the hydrogen atom and another the activated carbon fragment (Scheme 1).[2d−g] These systems have a preference for breaking aliphatic C−H bonds and are not reactive toward aromatic C−H bonds.[2a−c] Although these are interesting from an academic and mechanistic point of view, the thus-obtained "activated" hydrocarbons in the form of organometallic [R−Rh^{III}(por)] species lack reactivity because of the strong Rh−C bond. Furthermore, the only available site for further substrate binding is in the position trans to the hydrocarbon fragment R. Similar approaches using M^{II}(N-ligand) metalloradicals (M = Rh, Ir) with nonplanar N-ligands have not led to useful C−H bond transformations either,[3] as the M^{III}-containing products are coordinatively saturated and kinetically inert. On the contrary, the use of low-valent metalloradicals (e.g., Rh^0 or Ir^0) in binuclear C−H activations should become synthetically more useful because kinetically labile and thus reactive Rh^I−alkyl and Rh^I−H species are the expected primary products. However, "true rhodium(0) complexes" are rare, as most of them (on close inspection) actually prove to be highly delocalized radicals or "ligand radicals" having only a low spin density at the metal.[4] Consequently, most of them are not reactive toward C−H bonds, although there are some interesting (but poorly understood) exceptions.[5,6]

We recently reported the first well-documented example of a metal-centered Rh metalloradical: [Rh^0(trop$_2$PPh)(PPh$_3$)] (**1M**$^\bullet$).[7] This metalloradical exists as a clearly detectable species in rapid equilibrium with its "ligand radical" electromeric form **1L**$^\bullet$ (i.e., **1L**$^\bullet$ and **1M**$^\bullet$ are "redox isomers").[7]

1L$^\bullet$ and **1M**$^\bullet$ differ structurally only in their P_{trop}−Rh−P_{PPh3} angles (Scheme 2) but have very different electronic structures. The spin density of the thermodynamically slightly preferred electromer **1L**$^\bullet$ (E_{rel} = −2.0 kcal mol^{-1}) is strongly delocalized, and only ∼30% of the spin density is located at the metal. The other electromer **1M**$^\bullet$ shows 86% of the spin density in the Rh−P^{trop} bond, with ∼60% at the metal. Therefore, this radical can be regarded as a "Rh(0) complex".

Scheme 1. Binuclear Metalloradical C−H Bond Activation

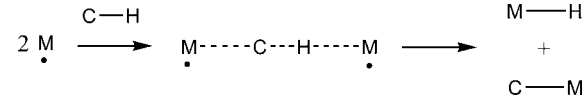

Scheme 2. Intermolecular C−H Bond Activation for **1L**$^\bullet$/**1M**$^\bullet$

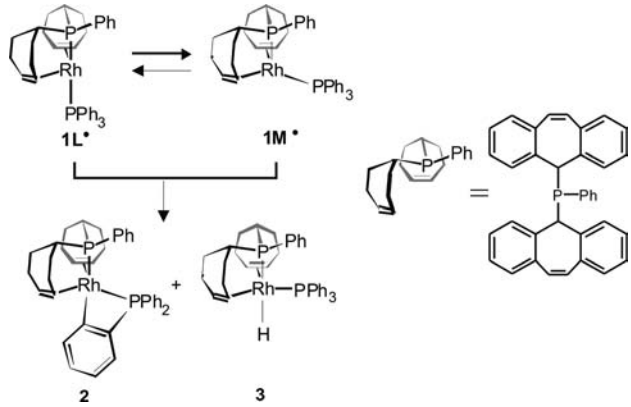

Here we show that PPh_3 dissociation from **1L**$^\bullet$/**1M**$^\bullet$ produces the reactive species **15e**, which reacts with the metalloradical **1M**$^\bullet$ to activate an aromatic C−H bond.

THF solutions containing a mixture of the radicals **1L**$^\bullet$ and **1M**$^\bullet$ (obtained cleanly upon one-electron reduction of the diamagnetic [Rh^I(trop$_2$PPh)(PPh$_3$)]$^+$ precursor) in the presence of 10 additional equiv of PPh_3 are fully stable for up to several days at room temperature.[7] In absence of additional PPh_3, we observed quantitative and selective conversion of the radical species to the diamagnetic Rh^I complexes **2** and **3** in a 1:1 ratio within 10 h at room temperature (Scheme 2).[8] The benzo-1-rhoda-2-phosphacyclobutane complex **2** is ortho-metalated at one of the aromatic rings of PPh_3, while the axial hydride complex **3** contains an unmodified PPh_3 ligand.

The X-ray structure of compound **2** is shown in Figure 1.[9] The structure of **2** is unique in the sense that all of the Rh complexes with ortho-metalated R_2P−Ph ligands reported to date in the Cambride Structural Database (CSD) have higher oxidation states.[10] Complex **2** is the first example that contains Rh^I.

The reaction of **1L**$^\bullet$/**1M**$^\bullet$ to form **2** and **3** could proceed via several possible mechanisms, so we decided to investigate the mechanism of this reaction in detail. The kinetics of the formation of **2** and **3** from the radicals **1L**$^\bullet$ and **1M**$^\bullet$ were measured by ^{1}H NMR spectroscopy. Experimental restrictions prevented us from following the decay of **1L**$^\bullet$/**1M**$^\bullet$ directly in a reliable way. However, the characteristic paramagnetically broadened ^{1}H NMR signals of **1L**$^\bullet$/**1M**$^\bullet$ at 10.90, 9.85, and 4.73 ppm (as well as their characteristic EPR signals) disappeared simultaneously with the appearance and buildup of the ^{1}H NMR signals of the diamagnetic products, so

[†] Universiteit van Amsterdam.
[‡] ETH-Hönggerberg.

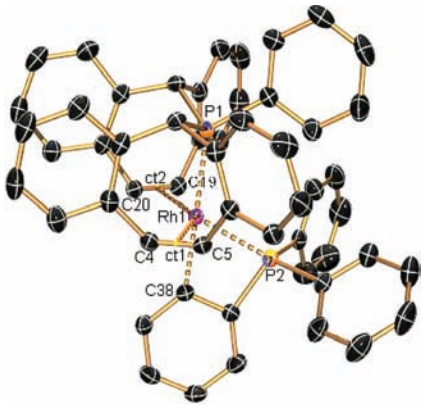

Figure 1. ORTEP plot (30% ellipsoid probability) showing the X-ray structure of **2**·$^1/_2Et_2O$. The diethyl ether solvent molecule and hydrogen atoms have been omitted for clarity. Selected bond lengths (Å) and angles (deg): Rh1−P1, 2.275(1); Rh1−P2, 2.382(1); Rh1−C38, 2.076(3); Rh1−C4, 2.185(3); Rh1−C5, 2.201(3); Rh1−C19, 2.171(3); Rh1−C20, 2.187(3); C4═C5, 1.414(3); C19═C20, 1.424(4); Rh1−ct1, 2.076(3); Rh1−ct2, 2.059(3); C38−Rh1−P1, 178.9(1); C38−Rh1−P2, 67.2(1); P1−Rh−P2, 113.9(1); ct1−Rh1−ct2, 132.9(1); ∑∠(C−P1−C), 310.9(4); ∑∠(C−P2−C), 319.7(4).

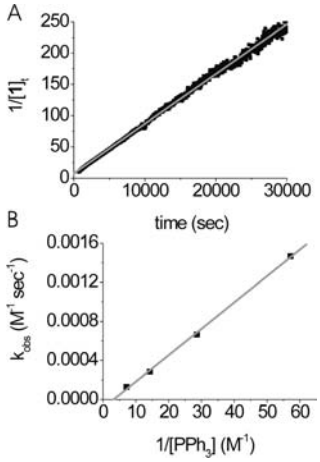

Figure 2. (A) Second-order kinetic plot for the reaction of **1**• to give species **2** and **3**. (B) Inverse-first-order behavior of the reaction rate with respect to the [PPh_3] concentration.

the kinetics could be conveniently followed by monitoring the appearance of species **2** and **3** with time ($[\mathbf{1}^\bullet]_t = 2[\mathbf{2}]_{final} - [\mathbf{2}]_t = 2[\mathbf{3}]_{final} - [\mathbf{3}]_t$), providing the following mechanistic information: (a) The rate of decay of **1**• is proportional to $[\mathbf{1}^\bullet]^2$, with a second-order rate constant $k_{obs} = 0.0067\ M^{-1}\ s^{-1}$ at 293 K (Figure 2A). (b) The lower relative decay rate of the radical [Rh(trop$_2$PPh)([D_{15}]PPh_3)] with the perdeuterated phosphane ligand reveals a kinetic isotope effect (KIE) of $k_H/k_D = 3.0$, thus indicating rate-limiting C−H bond activation. This reaction selectively produces D_{14}-**2** and D_{16}-**3**, the latter containing a deuteride (Rh−D) ligand. (c) When 0.25−2.0 molar equiv of PPh_3 is added, the reaction rate decreases and is inversely proportional to [PPh_3] (Figure 2B). (d) The activation parameters for the reaction **1**• → **2** + **3** were experimentally determined: $\Delta G^\ddagger = 25.8$ kcal mol^{-1}, $\Delta H^\ddagger = 12.6$ kcal mol^{-1}, and $\Delta S^\ddagger = -45.1$ cal mol^{-1} K^{-1} (the Eyring plot is shown in Figure S2 in the Supporting Information). The large negative activation entropy points to an ordered transition state, consistent with the second-order kinetics with respect to **1**•.

On the basis of these observations, we propose the mechanism shown in Figure 3, which includes: (1) dissociation of PPh_3 from **1L**•/**1M**• to give [Rh(trop$_2$PPh)] (**15e**) (k_1, k_{-1}, and $K_{eq1} = k_1/k_{-1}$);

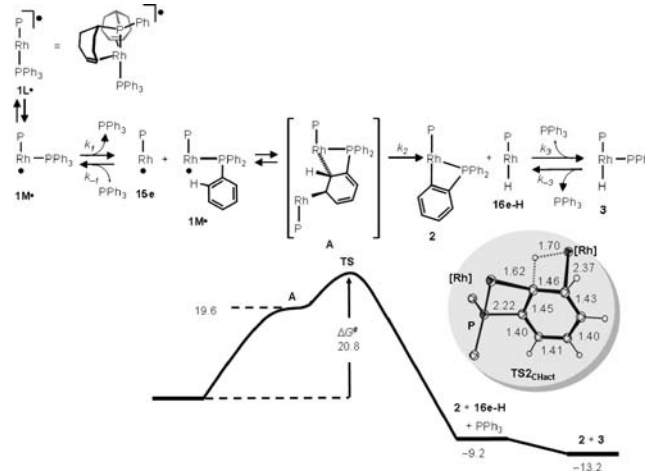

Figure 3. Computed minimum-energy reaction pathway (MERP) for formation of **2** and **3**. Relative free energies (DFT, bp86, TZVP, $T = 298$ K, $P = 1$ bar, corrected for the condensed-phase reference volume) in kcal mol^{-1}. Selected bond lengths (Å) of the **TS** are shown in the inset.

(2) reaction of this 15-electron radical **15e** with **1M**• in the rate-limiting H-transfer step to give rhodaheterocycle **2** and the unsaturated hydride *trans*-[RhH(trop$_2$PPh)] (**16e-H**) (k_2; this is the rate-limiting step); and (3) capture of free PPh_3 by the latter to give **3** (k_3, k_{-3}, and $K_{eq3} = k_3/k_{-3}$). The experimentally observed rate equation can be given as rate $= -d[\mathbf{1L}^\bullet]/dt = k_{obs}[\mathbf{1L}^\bullet]^2$, with $k_{obs} \approx k_2K_{eq1}[PPh_3]^{-1}$.

We performed additional density functional theory (DFT) calculations to shed some light on the nature of the rate-limiting step (see the Supporting Information for details), and the computed reaction path (with full molecules **1L**•, **1M**•, **2**, and **3)** at $T = 298$ K is shown in Figure 3.[11] The transition-state search for the hydrogen-transfer pathway was approached from the diamagnetic products side, causing the transition state (**TS**) to be connected with the diamagnetic high-energy intermediate **A**, but this species is likely the result of a computational artifact.[12] The potential energy surface around **A** is flat, and its fragmentation into the radicals **1M**• and **15e** is essentially barrierless. In that respect, the conversion of **1M**• and **15e** via **TS** to **2** and **16e-H** should be considered as a one-step process. Nonetheless, the addition of **15e** across a double bond of the PPh_3 fragment coordinated to **1M**• to produce species **A** with two Rh(I) centers and disruption of the arene structure of the bridging phenyl group as **1M**• and **15e** approach **TS** is strikingly similar to the formation of $M^{III}-CH_2-CH_2-M^{III}$ species through radical−radical coupling of M^{II} metalloradicals (M = Rh, Ir), as reported for [Rh^{II}(por)] and [Ir^{II}(Me_3tpa)] species upon reaction with ethene.[13] The C−H activation step via **TS** (see the inset in Figure 3) can be described as a β-hydrogen elimination reaction from **A**, producing species **2** and the 16-electron hydride species **16e-H**. Capture of PPh_3 completes the overall exothermic (−13.2 kcal mol^{-1}) reaction sequence. The computed mechanism agrees very well with the observed rate equation and conveniently explains the experimental KIE [$k_H/k_D = 3.0$ (exptl) and 3.1 (DFT)]. The calculated activation parameters ($\Delta G^\ddagger = 20.8$ kcal mol^{-1}, $\Delta H^\ddagger = 8.9$ kcal mol^{-1}, $\Delta S^\ddagger = -39.6$ cal mol^{-1} K^{-1} with respect to **1L**•) are in good agreement with the experimental data (which must in part be fortuitous), suggesting that the actual H-transfer process might indeed proceed as shown in Figure 3.

In conclusion, the results reported here indicate that the concerted action of two Rh^0 radicals with appropriate structures may very well be of use in bond activation chemistry. This reactivity is somewhat similar to bond activation processes observed for Rh^{II}

and Ir^{II} metalloradicals.[14] However, while activation of C═C or C−H bonds with M^{II} radicals typically produces kinetically inert M^{III} species, aromatic C−H bond activation with Rh^0 metalloradicals produces Rh^I−aryl and Rh^I−H species. The kinetic lability of **2** and **3** needs to be confirmed, but this is generally the case for Rh^I species. Therefore, binuclear oxidative addition of C−H bonds between two Rh^0 radicals may create interesting opportunities for follow-up reactivity. Current research is thus focused along these lines, aiming at the detection and use of 15-electron low-valent Rh^0 radicals for C−H functionalization.

Acknowledgment. The work was supported by the Swiss National Science Foundation (SNF), The Netherlands Organization for Scientific Research−Chemical Sciences (NWO-CW VIDI Project 700.55.426), the European Research Council (Grant Agreement 202886), the University of Amsterdam, and ETH Zürich.

Supporting Information Available: Experimental and computational details, coordinates of optimized geometries (PDB, XYZ), computed energies (XLS), and crystallographic data for **2** (CIF). This material is available free of charge via the Internet at http://pubs.acs.org.

References

(1) The various approaches include organometallic activation (oxidative addition and σ-bond metathesis/σ-complex-assisted metathesis mechanisms), (free) radical reactions, and carbene/carbenoid insertions. Some reviews of general interest: (a) Crabtree, R. H. *J. Chem. Soc., Dalton Trans.* **2001**, 2437. (b) Crabtree, R. H. *J. Organomet. Chem.* **2004**, *689*, 4083. (c) Slugovc, C.; Padilla-Martínez, I.; Sirol, S.; Carmona, E. *Coord. Chem. Rev.* **2001**, *213*, 129. (d) Klei, S. R.; Golden, J. T.; Burger, P.; Bergman, R. G. *J. Mol. Catal. A: Chem.* **2002**, *189*, 79. (e) Lersch, M.; Tilset, M. *Chem. Rev.* **2005**, *105*, 2471. (f) Sabo-Etienne, S.; Perutz, R. N. *Angew. Chem., Int. Ed.* **2007**, *46*, 2578. (g) Barton, H. R.; Hu, B. *Pure Appl. Chem.* **1997**, *69*, 1941. (h) Fokin, A. A.; Schreiner, P. R. *Adv. Synth. Catal.* **2003**, *345*, 1035. (i) Rowlands, G. J. *Annu. Rep. Prog. Chem., Sect. B.* **2008**, *104*, 19. (j) Campos, K. R. *Chem. Soc. Rev.* **2007**, *36*, 1069. (k) Díaz-Requejo, M. M.; Belderrain, T. R.; Nicasio, M. C.; Pérez, P. J. *Dalton Trans.* **2006**, 5559. (l) Davies, H. M. L. *Angew. Chem., Int. Ed.* **2006**, *45*, 6422. (m) Davies, H. M. L.; Manning, J. R. *Nature* **2008**, *451/24*, 417.

(2) (a) Del Rossi, K. J.; Wayland, B. B. *J. Am. Chem. Soc.* **1985**, *107*, 7941. (b) Del Rossi, K. J.; Wayland, B. B. *J. Chem. Soc., Chem. Commun.* **1986**, 1653. (c) Del Rossi, K. J.; Zhang, X.-X.; Wayland, B. B. *J. Organomet. Chem.* **1995**, *504*, 47. (d) Wayland, B. B.; Ba, S.; Sherry, A. E. *J. Am. Chem. Soc.* **1991**, *113*, 5305. (e) Sherry, A. E.; Wayland, B. B. *J. Am. Chem. Soc.* **1990**, *112*, 1259. (f) Wayland, B. B.; Ba, S.; Sherry, A. E. *Inorg. Chem.* **1992**, *31*, 148. (g) Zhang, X.-X.; Wayland, B. B. *Inorg. Chem.* **2000**, *39*, 5318. (h) Zhang, X.-X.; Wayland, B. B. *J. Am. Chem. Soc.* **1994**, *116*, 7897. (i) Cui, W. H.; Zhang, X. P.; Wayland, B. B. *J. Am. Chem. Soc.* **2003**, *125*, 4994. (j) Cui, W. H.; Wayland, B. B. *J. Am. Chem. Soc.* **2004**, *126*, 8266.

(3) (a) Hetterscheid, D. G. H.; Klop, M.; Kicken, R. J. N. A. M.; Smits, J. M. M.; Reijerse, E. J.; de Bruin, B. *Chem.—Eur. J.* **2007**, *13*, 3386. (b) Tejel, C.; Ciriano, M. A.; Passarelli, V.; López, J. A.; de Bruin, B. *Chem.—Eur. J.* **2008**, *14*, 10985.

(4) de Bruin, B.; Russcher, J. C.; Grützmacher, H. *J. Organomet. Chem.* **2007**, *692*, 3167.

(5) (a) Sofranko, J. A.; Eisenberg, R.; Kampmeier, J. A. *J. Am. Chem. Soc.* **1980**, *102*, 1163. (b) Pilloni, G.; Zotti, G.; Zecchini, S. *J. Organomet. Chem.* **1986**, *317*, 357. (c) Mueller, K. T.; Kunin, A. J.; Greiner, S.; Henderson, T.; Kreilick, R. W.; Eisenberg, R. *J. Am. Chem. Soc.* **1987**, *109*, 6313.

(6) Abstraction of "hydrogen atoms" from MeOH (fast) and CH_3CN (slow) reported for $[Rh^0(dppe)_2]$ proceeds via disproportionation of Rh^0 to Rh^{+1} and Rh^{-1} followed by protonation of Rh^{-1} to give Rh^{+1}−H: Kunin, A. J.; Nanni, E. J.; Eisenberg, R. *Inorg. Chem.* **1985**, *24*, 1852.

(7) Puschmann, F. F.; Harmer, J.; Stein, D.; Rüegger, H.; de Bruin, B.; Grützmacher, H.; *Angew. Chem., Int. Ed.* [Online early access]. DOI: 10.1002/anie.200903201. Published Online: Dec 2, 2009.

(8) A small amount (5−10%) of the equatorial hydride $[Rh(H_{eq})(trop_2PPh)(PPh_3)_{ax}]$ (**3′**), probably resulting from a side reaction with traces of H_2O, was also detected (see the Supporting Information).

(9) Crystal structure of $[Rh((C_6H_4)PPh_2)(trop_2PPh)]\cdot{}^1/_2Et_2O$ (**2**): Yellow single crystals were obtained from slow evaporation of a diethyl ether solution of **2**; $C_{56}H_{46}O_{0.5}P_2Rh$; triclinic; space group $P\bar{1}$; $a = 12.245(3)$ Å, $b = 14.106(3)$ Å, $c = 15.104(3)$ Å, $\alpha = 63.58(3)°$, $\beta = 78.33(3)°$, $\gamma = 66.59(3)°$; $V = 2143.1(8)$ Å^3; $Z = 2$; $\rho_{calcd} = 1.382$ g m^{-3}; crystal dimensions $0.12 \times 0.10 \times 0.05$ mm^3; Bruker SMART K1 diffractometer with CCD area detector; Mo Kα radiation ($\lambda = 0.71073$ Å), 200 K, $2\Theta_{max} = 56.63°$; 10598 reflections, 8995 independent ($R_{int} = 0.0421$); direct methods; empirical absorption correction using SADABS version 2.03; refinement against full matrix (vs F^2) with SHELXTL version. 6.12 and SHELXL-97; 543 parameters; R1 = 0.0392, wR2 (all data) = 0.0857; max/min residual electron density 0.647/−0.457 e Å^{-3}. All non-hydrogen atoms except those assigned to the disordered diethyl ether solvent molecule were refined anisotropically. The contribution of the hydrogen atoms, in their calculated positions, was included in the refinement using a riding model. The strongly disordered diethyl ether solvent molecule was described by 6.6 carbon atoms (C55−C61), corresponding to 39.6 electrons (one diethyl ether molecule contains 42 electrons). The crystallographic data for **2** (excluding structure factors) has been deposited with the Cambridge Crystallographic Data Centre (CCDC) as supplementary publication no. CCDC-706732. Copies of the data can be obtained free of charge on application to CCDC, 12 Union Road, Cambridge CB2 1EZ, U.K. [fax: (+44) 1223-336-033; E-mail: deposit@ccdc.cam.ac.uk).

(10) The CSD reports 26 M^{III} examples (M = Rh, Ir) but only a single report claiming Ir^I examples (ref 10d). However, these were poorly characterized (only X-ray diffraction data), so we cannot exclude the possibility that these are actually also $Ir^{III}H$ species. Selected examples: (a) Cooper, A. C.; Clot, E.; Huffman, J. C.; Streib, W. E.; Maseras, F.; Eidenstein, O.; Caulton, K. G. *J. Am. Chem. Soc.* **1999**, *121*, 97. (b) Cao, C.; Wang, T.; Patrick, B. O.; Love, J. A. *Organometallics* **2006**, *25*, 1321. (c) Bennet, M. A.; Bhargava, S. K.; Ke, M.; Willis, A. C. *J. Chem. Soc., Dalton Trans.* **2000**, 3537. (d) Perego, G.; Del Piero, G.; Cesari, M.; Clerici, M. G.; Perrotti, E. *J. Organomet. Chem.* **1973**, *54*, C51.

(11) We also considered more classical ortho-metalation reaction pathways. In the present case, these would involve the intramolecular oxidative addition of an ortho C−H bond of the P-phenyl group to the low-valent rhodium center of **1L**˙ or **1M**˙. However, these reactions lead to considerably higher energy species than those in the mechanism proposed here.

(12) The DFT orbital symmetry does not easily break spontaneously on going from a closed-shell singlet to an open-shell singlet solution. In that respect, species **A** is unlikely to be experimentally observable but rather a species close to the point along the reaction coordinate where the spin state changes in the approach of the radicals towards **TS**.

(13) (a) Wayland, B. B.; Sherry, A. E.; Pozmik, G.; Bunn, A. G. *J. Am. Chem. Soc.* **1992**, *114*, 1673. (b) Hetterscheid, D. G. H.; Kaiser, J.; Reijerse, E.; Peters, T. P. J.; Thewissen, S.; Blok, A. N. J.; Smits, J. M. M.; de Gelder, R.; de Bruin, B. *J. Am. Chem. Soc.* **2005**, *127*, 1895.

(14) Recent reviews covering the reactivity of Rh-, Ir-, Pd-, and Pt-based radicals: (a) de Bruin, B.; Hetterscheid, D. G. H.; Koekoek, A. J. J.; Grützmacher, H. *Prog. Inorg. Chem.* **2007**, *55*, 247. (b) de Bruin, B.; Hetterscheid, D. G. H. *Eur. J. Inorg. Chem.* **2007**, 211.

JA909022P